Stability and Structure of Protonated Clusters of Ammonia and Water, $H^+(NH_3)_m$ $(H_2O)_n$

Preben Hvelplund,*,† Theo Kurtén,*,‡,§ Kristian Støchkel,† Mauritz Johan Ryding,‖ Steen Brøndsted Nielsen,† and Einar Uggerud*,⊥

Department of Physics and Astronomy, Aarhus University, Ny Munkegade, Bld. 1520, DK-8000 Aarhus C, Denmark, Department of Physical Sciences, University of Helsinki, P.O. Box 64, FIN-00014 University of Helsinki, Finland, Department of Chemistry, H. C. Ørsted Institute, University of Copenhagen, Denmark, Department of Chemistry, Atmospheric Science, University of Gothenburg, SE-412 96 Göteborg, Sweden, and Mass Spectrometry Laboratory and The Centre for Theoretical and Computational Chemistry, Department of Chemistry, University of Oslo, P.O. Box 1033 Blindern, N-0315 Oslo, Norway

Received: May 7, 2010; Revised Manuscript Received: June 11, 2010

Mass spectrometric experiments show that protonated mixed ammonia/water clusters predominant exist in three forms namely $H^+(NH_3)_4(H_2O)_n$, $H^+(NH_3)_5(H_2O)_n$, and $H^+(NH_3)_6(H_2O)_n$ ($n = 1-25$). For the first two series the collisional activation mass spectra are dominated by loss of water, whereas ions of the latter series preferably lose ammonia. The quantitative characteristics of these observations are reproduced by quantum chemical calculations that also provide insight into the geometrical structures of the clusters. Although the experiments and the calculations agree that clusters with five ammonia are thermodynamically preferred, this does not indicate a rigid tetrahedral structure with one central ammonium covered with an inner solvation shell of four ammonia molecules, with water outside. Instead, water and ammonia have comparable affinities to the binding sites of the first shell, with a preference for ammonia for the first two sites, and water for the last two. The "leftover" ammonia molecules bind equally strong as water molecules to sites in the second shell due to synergistic hydrogen binding. Finally, it is discussed whether the observation of enhanced stability of the $H^+(NH_3)_5(H_2O)_{20}$ in terms of magic numbers and associated geometries may be related to a tetrahedral ammonium core encapsulated in a dodecahedral $(H_2O)_{20}$ structure, typically found in clathrates.

Introduction

Molecular clusters of water, $(H_2O)_n$, are attractive small-scale model systems that provide valuable insight into the structure and dynamics of bulk water and a wide range of phenomena associated with water.[1] For example, by introducing one or more ionic or neutral molecules into a cluster, it becomes possible to investigate solvation in water at a fundamental level. Water clusters, in particular ionic water clusters, have been extensively studied for many decades using mass spectrometry, and introduction of the high pressure, supersonic expansion, and electrospray sources has been determining for the scientific development in this field.[2,3] The physical and chemical properties of water clusters are also relevant to atmospheric chemistry since they correspond to critical stages in naturally occurring processes that involve nucleation and growth of water-containing droplets and particles.[4] Ions are very effective in nucleation, although the importance of ions relative to other nuclei in tropospheric nucleation is debated.[5] Ions are formed in the lower atmosphere via a number of mechanisms, including the effect of high energy cosmic radiation.[6,7] The latter mechanism has been suggested to influence global cloud cover, and thereby the climate.[8] Among the many substances found in the atmosphere, ammonia is significant due to its relatively high basicity, which makes it a potential proton sink, thereby forming an ionic nucleation center.[9,10] It is interesting and relevant that the complex $NH_4^+(H_2O)_2$ was already identified in ground-level atmosphere in 1984.[9] It should also be mentioned that ammonia and sulphuric acid, both atmospheric trace gases, together are much more potent in nucleation than each constituent apart.[11]

For these and other reasons, a large number of experimental and computational investigations of protonated clusters of ammonia and water have been conducted in the past. Kebarle et al. were early in studying protonated water clusters[12] and protonated ammonia clusters[13] applying a high pressure ion source. From these and later studies from many laboratories it has emerged that $H^+(H_2O)_n$ and $H^+(NH_3)_n$ are structurally rather different.

In pure $H^+(NH_3)_m$, both thermochemical[13–16] and spectroscopic data,[17–19] as well as computational studies,[20–23] indicate a shell structure. The proton is bonded to a central ammonia molecule, and the so formed tetrahedral ammonium ion serves as the core ion providing hydrogen bonding to four equivalent ammonia molecules forming the first solvation shell. Further shells appear to be formed around this first solvation sphere.

In pure protonated water clusters the situation is more complex.[24,25] The preferred geometry of $H^+(H_2O)_4$ is a central hydroxonium core with three waters attached by hydrogen bonding, forming a trigonal structure. On this basis, the network of water molecules forms sheets rather than space filling structures, at least for smaller clusters. Pentagons and hexagons of water are typical structural elements for medium-sized clusters.[26] In addition to this structural complexity, one also has to take into account the fact that besides having a central H_3O^+ (the Eigen-structure), there also exist clusters centered around the alternative Zundel-structure, $H^+(H_2O)_2$, in which the bridging

* To whom correspondence should be addressed. E-mail: hvelplun@phys.au.dk (P. H.), theo.kurten@helsinki.fi (T. K.), einar.uggerud@kjemi.uio.no (E. U.).
† Aarhus University.
‡ University of Helsinki.
§ University of Copenhagen.
‖ University of Gothenburg.
⊥ University of Oslo.

10.1021/jp104162k
Published on Web 06/22/2010

proton is equally shared between two water molecules. This has been inferred from spectroscopy.[25] Molecular dynamics simulations have indicated that the energy difference between the two types of clusters is small and proton migration is swift,[27] a condition that is also found from isotope exchange experiments with $H^+(H_2O)_n$ clusters.[28] It was noted by Lin that mass spectra of protonated water molecules contain peaks with enhanced intensity at $n = 21$ and 28, suggesting particularly stable configurations ("magic numbers").[29] The enhanced stability of $n = 21$ was explained by Searcy and Fenn to stem from the pentagonal dodecahedron, as found in methane clathrates, with the hydroxonium ion at the center of the cage.[30] More recently, this has been shown to be a very unlikely explanation, since the closed dodecahedral structure is high in energy compared to other structures, in particular the edge-sharing pentagonal prism.[31,32,24,33]

Superficially, protonated clusters consisting of both ammonia and water appear to have more in common with pure clusters of ammonia than pure clusters of water. In $H^+(NH_3)(H_2O)_n$, with $n = 0-5$, it has been inferred from the thermochemistry of water ligand binding[34] and by spectroscopy and computation[35] that the geometry is in accordance with a central ammonium ion surrounded with water, of which four occupy the first shell. From intensity variations in high pressure mass spectra, Hogg and Kebarle suggested that in mixed clusters of the type $H^+(NH_3)_m(H_2O)_n$ there is a central $H^+(NH_3)_5$ motif as found for protonated pure ammonia clusters.[13,14] It also appeared that water molecules have higher affinity for the second shell than ammonia molecules. Shinora et al. investigated water−ammonia clusters $H^+(NH_3)_m(H_2O)_n$ with $m + n < 40$ applying electron impact ionization or photoionization to neutral clusters formed by supersonic expansion.[36–38] They found no clusters with more than six ammonia molecules, suggesting thermodynamic preference for water in the outer shells. In addition, they identified clusters containing 20 water molecules with $m = 1-6$ to have enhanced stability (corresponding to magic numbers). Moreover, the same authors identified both $H^+(NH_3)_4(H_2O)$ and $H^+(NH_3)_5$, indicating competition between ammonia and water even for sites in the first solvation shell.[36]

We present results of a new investigation of $H^+(NH_3)_m(H_2O)_n$ clusters applying an atmospheric chemical ionization cluster source and observing stability patterns and relative evaporation tendencies from recorded mass spectra, thereby complementing previous experimental efforts. The goal of our study is to understand the structural and thermochemical factors that determine the relative affinity of water and ammonia to the different positions in the first and second solvation shells around NH_4^+. To support the interpretation and to provide the necessary structural insight we have conducted a series of high-level quantum chemistry calculations.

Experimental Section

The ion source is described in detail elsewhere.[39–42] It is located on a platform floating at a potential of 50 kV and was operated in discharge mode to produce protonated ammonia/water clusters, $H^+(NH_3)_m(H_2O)_n$ in an atmosphere resulting from bubbling air through a gas-washing flask containing 25% ammonia in water (Merck p.a.). The bubbling results from the low pressure in the region where the plasma/gas is injected into the vacuum of the mass spectrometer. The ion source conditions were controlled to produce clusters with $m + n$ ranging from 1 to 100, in particular the temperature of the heated capillary (40−60 °C) and the voltage of the tube lens located between the capillary and a skimmer were optimized. The ions were let through a differentially pumped lens system before they were accelerated to 50 keV. The instrument used for the experiments is a home-built double sector mass spectrometer with BE geometry (B = magnetic sector, E = electric sector). Ions of interest were then separated according to m/z value by a 72° sector magnet having a radius of curvature of 2 m. In the CID experiments, the ions were passed through a collision cell filled with air at nominal $p = 4 \times 10^{-5}$ mbar giving 30% reduction of the primary ion beam intensity. The resulting swarm of ions was allowed for energy analysis by a 180° hemispherical electrostatic analyzer with a radius of curvature of 15 cm, resulting in a fragment mass spectrum. Ion counting was accomplished using a channeltron detector (Ceratron-E (muRata Japan)). A linear calibration between analyzer voltage (voltage difference between the two analyzer plates) and m/z was done based on the two end points, 0.0 and 10.4 kV, corresponding to m/z values of zero and the m/z of the parent ion, respectively.

Computational Details. All calculations were performed using the Gaussian 09 program suite[43] and the CBS-QB3 method.[44,45] CBS-QB3 is a composite method involving geometry optimizations and vibrational frequency calculations with the B3LYP functional and a triple-ζ basis set, followed by a series of energy calculations aiming at estimating the CCSD(T) energy in the complete basis set limit. Errors in vibrational frequencies and the imbalance of electron spin contributions are accounted for by using empirical scaling factors. For a test set of single molecules, the CBS-QB3 binding energies are accurate to within about 1 kcal/mol, around 4 kJ/mol.[45] For molecular clusters, the accuracy of the computed energies is presumably somewhat lower, but still significantly more accurate than methods applied in previous studies of protonated ammonia−water clusters. For the systems studied here, the largest errors are probably not related to the electronic energy calculations but stem from the rigid rotor-harmonic oscillator approximation used in calculating the thermal contributions to the enthalpies and, in particular, the entropies. For the larger clusters in this study, especially the structures corresponding to the lowest Gibbs free energy values, the minimum vibrational wavenumbers were often in the $2-4$ cm^{-1} range, and animation of the vibrational eigenmodes showed them to correspond to essentially free relative rotations of NH_3 molecules rather than bonded vibrations. In addition, an entropy term also arises from the fact that equivalent ligand positions give rise to a symmetry factor, which has to be accounted for during evaporation processes.[46] Although this in principle is a simple task, in practice only a maximum and a minimum value could be identified for each cluster size due to the complexity associated with multiple low-lying isomers. This introduces an additional uncertainties of ±2 kJ/mol. For these reasons, free energy estimates computed using the harmonic approximation should therefore be considered to be essentially qualitative. When there are several isomers of low energy, the free energy estimates may have additional uncertainties.

Due to the computational effort involved in the CBS-QB3 calculation (especially the triples contribution in the CCSD(T) step, which scales as the seventh power of the system size), our calculations are restricted to clusters containing eight molecules or less. This, combined with the structural information presented in previous studies[21–23] of protonated pure ammonia clusters (and reconfirmed here), allows the configurational sampling of the clusters to be carried out manually, that is, by explicitly constructing the input geometries rather than obtaining them by an automated method. (We also attempted force-field based structure sampling using standard doctrines for force-

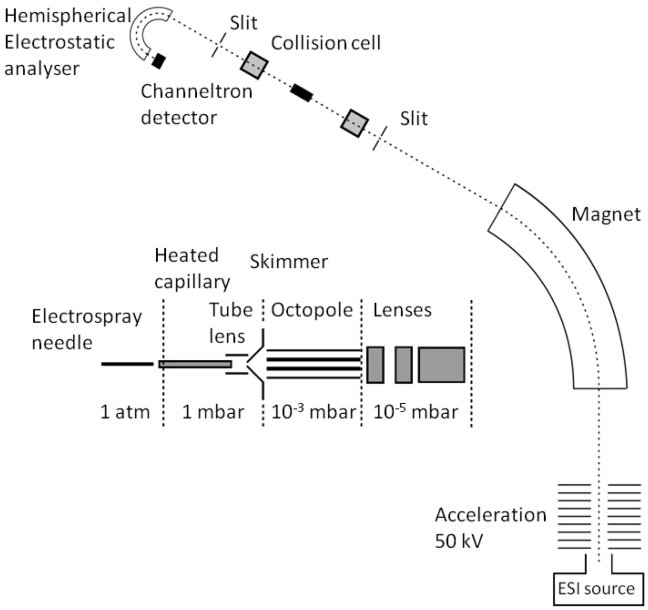

Figure 1. Schematic outline of the instrument used.

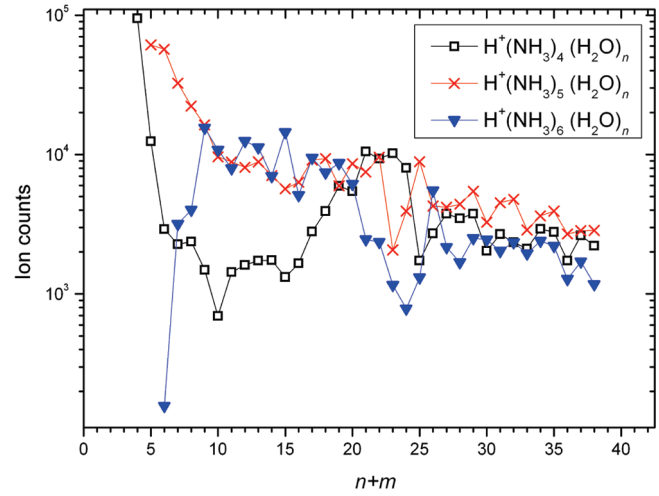

Figure 2. Ion counts recorded during scanning of the magnetic sector in terms of the total number of water and ammonia molecules, $n + m$.

field generation, but these gave the same minimum energy structures as manual sampling.) The first five molecules in the cluster always formed a regular and fairly rigid structure, with 0−4 ligands arranged in a first solvation shell around a central NH_4^+ core ion, and no interligand hydrogen bonds. Thus, configurational sampling was only necessary for the 6−8 molecule clusters, and even then involved only a limited number of permutations for swapping H_2O and NH_3 molecules in the first shell, as well as arranging the 1−3 remaining second-shell ligands in different bonding patterns (e.g., various types of ring and cage structures). On the basis of our sampling, the "rule-of-thumb" of no interligand bonding in the first shell seems to hold fairly well even in the larger clusters, with the sole exception of the 1-water clusters containing first-shell water molecules H-bonded from both of their hydrogen atoms. In these cases, an adjacent first-shell NH_3 was always bent toward the water oxygen to form a ring structure. For the largest clusters with more than one water molecule, the lowest-enthalpy structures contained one water in the second shell, as well as multiple ring structures, whereas the lowest free-energy structures (with one exception) contained all waters in the first shell and few or no rings. This is most likely due to the unfavorable entropy contribution associated with ring formation.

For each cluster structure with more than 5 molecules, multiple structural isomers could always be found. For the largest 7 and 8 molecule clusters with 2 or 3 water molecules, around 10 different input structures were investigated for each stoichiometry, although not all trial geometries resulted in distinct, converged local minima. Our focus here has been on obtaining representative minimum-enthalpy and minimum-free energy structures; the sampling may not be complete with respect to high-energy isomers.

The energy, enthalpy or free energy differences between isomers differing only by internal rotations of NH_3 groups, or by the relative orientation of singly bonded second-shell ligands remote from reach other, were sometimes as low as 0.1 kJ/mol. However, we caution that these species should not really be considered as distinct, true structural isomers, even though application of the rigid rotor-harmonic approximation requires this assumption to be made. Isomers differing in their H-bonding patterns (for example, having a different number or different types of ring structures) were usually separated by between 3 and 20 kJ/mol with respect to the enthalpy, reflecting the differences in the strengths of H-bonds in these systems. Free energy differences tended to be somewhat larger than enthalpy differences, reflecting the greater sensitivity of the calculated entropies toward the precise bonding patterns. To the extent that the computed free energies are trustworthy, these results indicate that the room-temperature populations of structural isomers with bonding patterns significantly different from the identified global minima are fairly small, though not necessarily negligible.

Results

Mass Spectrum. The mass spectrum is dominated by four series of clusters, for which the chemical compositions are easily identified. At low masses, $m/z < 87$, we observe only neat ammonia clusters of the type $H^+(NH_3)_m$, with $m = 0-5$. This series terminates strictly at $m = 5$, with no observable neat cluster beyond that size. At higher masses, up to $(m + n) \leq 26$ we find significant peaks resulting from mixed clusters of three series only, $H^+(NH_3)_6(H_2O)_n$, $H^+(NH_3)_5(H_2O)_n$, and $H^+(NH_3)_4(H_2O)_n$. We have concentrated our efforts to the analysis of clusters having $m/z < 470$, that is, with $(m + n) \leq 26$. The three-cluster series continue far beyond $m/z = 470$, but no attempt to quantify relative intensities for these larger clusters was made due to limited mass accuracy and resolution, which makes peak assignment somewhat uncertain. For the clusters analyzed in detail (see Figure 2) we note that the $m = 5$ series gives rise to intense signals for each value of $(m + n)$, and in most cases this series is dominating. For $(m + n) = 10$, 12, 13, and 15, the most intense signal is for $m = 6$, whereas for the range 21−24 it is for $m = 4$. Regarding the relationship between $m = 4$ and $m = 6$, we notice that the latter is relatively more intense for the smaller clusters, gradually growing from being absent for $n = 0$ to being most abundant for $n = 5$. Quite extraordinarily, we observe that the most significant peak (>90%) for $(m + n) = 25$ is for $H^+(NH_3)_5(H_2O)_{20}$.

Collision-Induced Decomposition of Size Selected Clusters. CID experiments were performed systematically for ions with $m = 4-6$ and $n = 1-6$ plus other selected ions. The results are displayed in Figure 3. The observations are unambiguous in the sense that mixed cluster ions containing six ammonia molecules in one ligand dissociation preferably lose ammonia,

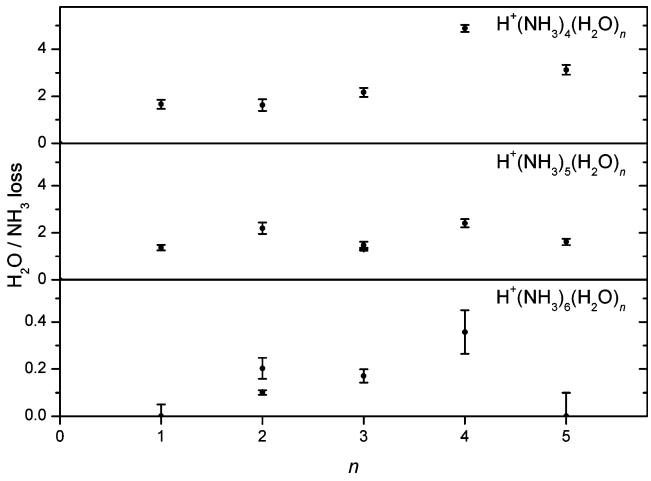

Figure 3. Results of CID experiments with size-selected $H^+(NH_3)_m(H2O)_n$ clusters ($m = 4-6$, $n = 1-6$) showing the fraction of dissociations leading to loss of H_2O relative to loss of NH_3. Note the finer grading of the *y*-axis in the bottom panel.

in the cases of $n = 1$, 3, and 5 almost exclusively, whereas those with 4 or 5 ammonia prefer to lose water. This rule is obeyed for all clusters sizes investigated, also those with $m + n > 12$. Due to the particularities of the cluster with $m = 5$ and $n = 20$ observed in the normal mass spectrum (see the paragraph above), this species was also the focus for CID experiments in which the ions $H^+(NH_3)_6(H_2O)_{20}$ and $H^+(NH_3)_5(H_2O)_{21}$ were selected. It turned out that the former exclusively (>96%) loses one ammonia, whereas the latter exclusively (>96%) loses one water in one ligand dissociation.

Computed Structures of $H^+(NH_3)_m$ ($m = 1-8$) Clusters. As already noted, the structures of $H^+(NH_3)_m$ clusters ($m = 1-8$) are well studied and understood.[21–23] The extra proton has been found to be clearly localized to one ammonia, with the other ammonia molecules binding as ligands to the so-formed ammonium core ion. Computational and experimental evidence has so far ruled against any clusters containing proton-bridged geometries similar to the Zundel structure (i.e., $N_2H_7^+$ or similar). The four first NH_3 ligands bind directly to the NH_4^+ core, with the subsequent ones forming a second shell. The minimum-enthalpy structures of the protonated pure ammonia clusters do not contain any ring structures. Concerning the detailed structures, our results are in full agreement with previous studies, and need not be discussed further here.

Computed Structures of $H^+(NH_3)_m(H_2O)$, $m = 1-7$. The optimum nuclear configurations for the $H^+(NH_3)_m(H_2O)$ clusters are shown in Figure 4. For $m < 5$, there are no surprising features: the global minima are obtained by geometry optimization after replacing one ammonia by one water molecule in the corresponding pure protonated ammonia cluster. For $m = 5$, the most stable geometrical structure (with respect to both enthalpy and free energy) contains one water molecule in the first hydration shell, with an ammonia molecule displaced to the second shell. The enthalpy and free energy difference to the thermodynamically less stable $m = 5$ isomer with water in the second shell are 6.5 and 22.9 kJ/mol, respectively. The same pattern is seen for the $m = 6$ and 7 clusters, although the presence of multiple second-shell ligands now allows for more structural diversity. The relative stabilities for the $m = 6$ and 7 cases depend on whether the comparison is made in terms of enthalpy or free energy. The minimum-enthalpy structures have two second-shell ammonia ligands bonded to the water molecule, with one first-shell ammonia tilted toward the water oxygen, forming an H-bonded ring structure. The minimum-enthalpy $m = 7$ configuration further contains a second ring structure, with one second-shell ammonia bonded to both a first-shell ammonia and one of the other second-shell ammonia molecules. As ring structures are unfavorable with respect to the entropy, the minimum free-energy geometries contain one less ring (i.e., zero rings for $m = 6$ and one ring for $m = 7$), and have one second-shell ammonia bonded to a first-shell ammonia far from the water molecule. The minimum free-energy $m = 7$ geometry has one first-shell ammonia tilted toward the water molecule.

Computed Structures of $H^+(NH_3)_m(H_2O)_2$, $m = 1-6$. The optimized cluster geometries for $H^+(NH_3)_m(H_2O)_2$ are shown in Figure 5. As above, the geometries of the clusters with $m < 4$ are as expected, since they contain only first-shell ligands bonded to the core ion, having no ring structures. The $m = 1$ geometry is similar to that found by Jiang et al.[35] For $m = 4-6$, the minimum-enthalpy structures contain one water molecule in the first shell, with the second water acting as a double H-bond acceptor in a four-membered ring. For $m = 5$ and 6, the additional ammonia molecules then add to this water molecule, in effect forming the beginning of a third shell of ligands. For $m = 4$ and 5, the minimum free energy structures are different from the minimum-enthalpy structures and contain both water molecules in the first shell (with the second-shell ammonia molecules binding to these waters). The enthalpy difference between the two $m = 4$, $n = 2$ structures shown in Figure 5 is only 1.5 kJ/mol, whereas the free energy difference is 13.6 kJ/mol. Similarly, the enthalpy and free energy differences between the two $m = 5$, $n = 2$ structures are 3.2 and 17.4 kJ/mol, respectively. For the $m = 6$, $n = 2$ cluster, the lowest enthalpy and lowest free energy local minima with two waters in the first shell (not shown) were 7.1 and 3.0 kJ/mol above the structure shown in Figure 5.

Computed Structures of $H^+(NH_3)_m(H_2O)_3$, $m = 1-5$. The geometries of the three-water clusters shown in Figure 6 are mostly of the same types as in the one- and two-water clusters described above. The $m = 1$ geometry is similar to that found by Jiang et al.[35] The $m = 1$ and 2 clusters resemble the pure ammonia clusters, with three ammonia molecules replaced by water, whereas the minimum-enthalpy isomers for $m = 3-5$ contain more ring structures than the minimum free-energy isomers. The lowest-enthalpy $m = 3$ structure resembles the corresponding $H^+(NH_3)_4(H_2O)_2$ cluster, with one water molecule acting as a double H-bond acceptor. For $m = 4$ and 5, the lowest-enthalpy structures contain a "cage" formed from two first-shell water molecules, one first-shell ammonia, one second-shell water, and one second-shell ammonia. The additional ammonia molecule in the $m = 5$ structure binds to a second-shell water, as observed for the two-water clusters above. The minimum free-energy structures for $m = 3-5$ all contain three water molecules in the first shell (as opposed to two for the lowest-enthalpy structures), with the additional ammonia molecules binding to these waters without any entropy-increasing ring structures. The second-shell ammonia molecules in $m = 4$ and 5 are all bonded to different water molecules, as observed for the two-water clusters. Similarly to the $n = 2$ clusters, the computed enthalpy differences between the structural isomers shown in Figure 6 were significantly smaller than the free energy differences. The enthalpy differences between the two depicted isomers were 0.8, 12.9, and 15.0 kJ/mol for the $m = 3$, 4, and 5 clusters, respectively. The corresponding free energy differences were 19.1, 35.6, and 34.4 kJ/mol, respectively. For the $m = 5$, $n = 3$ cluster, an additional isomer (not shown) with two

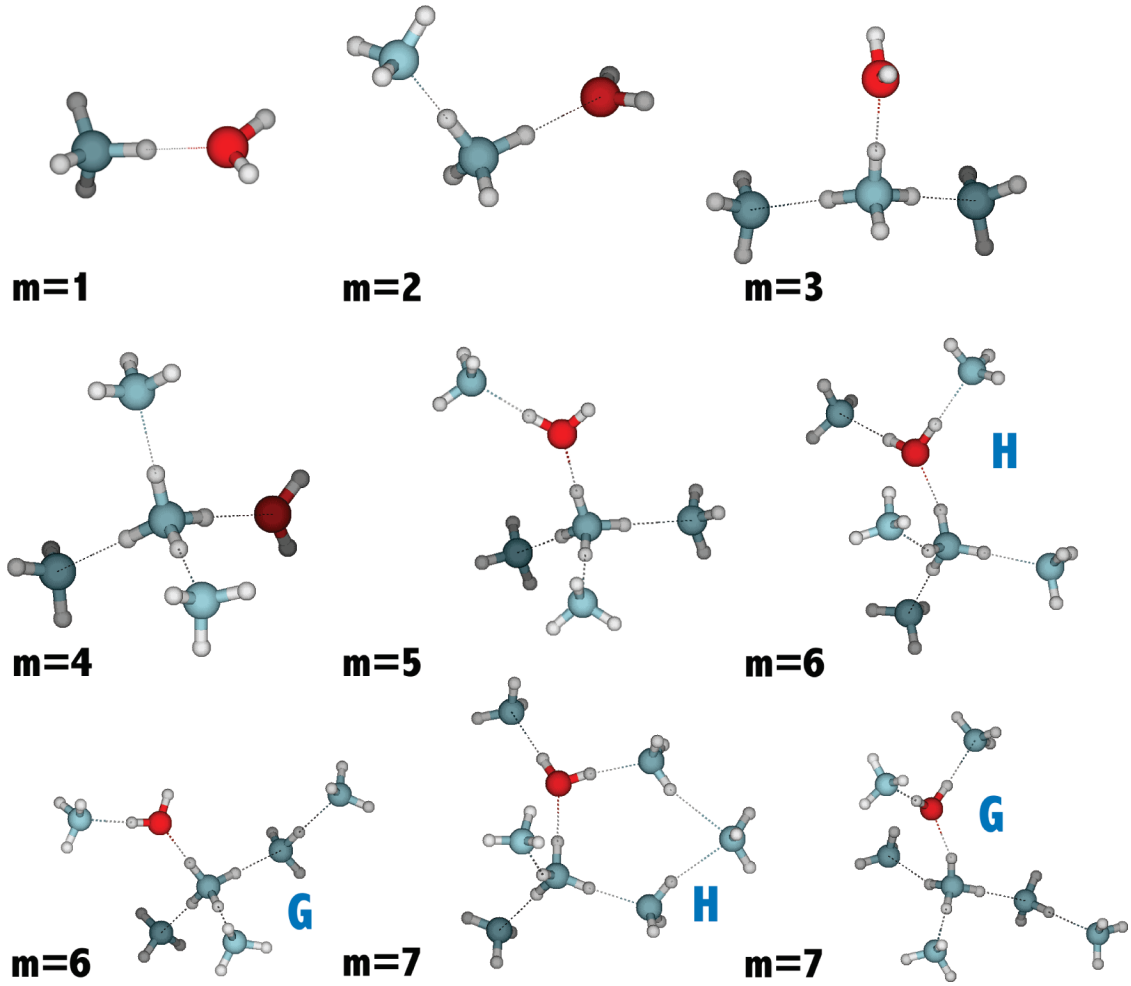

Figure 4. Minimum-enthaply and minimum-free energy structures (at 298 K and 1 atm reference pressure) for $H^+(NH_3)_m(H_2O)$ ($m = 1-7$) clusters. In the case that the most stable structure with respect to the enthalpy (H) and Gibbs free energy (G) were different, both are shown, and the letters "H" and "G" are used to denote the two isomers.

water molecules in the first shell was found that was only 5.7 kJ/mol above the presented lowest-G structure in free energy. However, the lowest vibrational frequency of this structure was only 4.6 cm^{-1}, rendering the computed entropy questionable. For the $m = 4$, $n = 3$ cluster, the minimum-entalpy structure at 0 K (not shown, but coordinates given in the Supporting Information) differs slightly from that at 298 K, in that the second-shell water molecule acts as a double acceptor to H-bonds from both the first-shell water molecules, and as a H-bond donor to a third-shell ammonia. This third-shell ammonia is not bonded to any other molecule in the cluster. At 298 K, this structure is less stable than the presented minima by 2.2 kJ/mol in enthalpy and 11.7 kJ/mol in free energy.

Enthalpies and Free Energies of Evaporation. The enthalpies and Gibbs free energies of evaporation of ammonia and water from the studied clusters are reported in Figures 7 and 8. The one-, two,- and three-water cluster series are plotted separately. Due to the effect of the very low wavenumber vibrations on the entropies, the free energy curves should be considered qualitative only; the enthalpy curves are likely to give a more reliable picture of the relative stabilities of the clusters and certainly so at lower temperatures. Despite the fact that the detailed shapes of the six curves differ, the general pattern is the same: the smaller clusters prefer to lose water, whereas the larger clusters prefer to lose ammonia. The crossover points occur between 5 and 6 ammonia molecules for the 1- and 2-water clusters, corresponding very precisely to the experimentally observed pattern. For the three-water clusters, the crossover point occurs between 4 and 5 ammonia molecules in the enthalpy curve, while the free energy curve has no crossover point. This corresponds qualitatively to the very small concentrations of $H^+(NH_3)_m(H_2O)_3$ (with $m < 6$) clusters seen in the experimental data.

Discussion

The clusters were generated in a corona discharge source operated under ambient conditions and introduced into the mass spectrometer via a capillary and further into the high vacuum via several stages of differential pumping. Inside the vacuum chamber the clusters are free to evaporate and the effective temperature of a given cluster will decrease for each ligand that is lost.[41] For this reason the exact energy content of each member of the cluster population observed in the magnet scan is not known. However, a reasonable estimate is $T = 150-200$ K.[47] Although the system is, strictly speaking, not in chemical or thermodynamic equilibrium, the mass spectrum collected for the evaporative ensemble reflects chemical stability in a rather straightforward manner, in particular regarding relative intensities of related species.[48] Nevertheless, it is assuring that our data and those obtained using high pressure chemical ionization[14] or ionization of a supersonically cooled gas[36–38] provide similar conclusions, namely, that there is a preference for protonated water/ammonia clusters with 5 ammonia molecules. In addition,

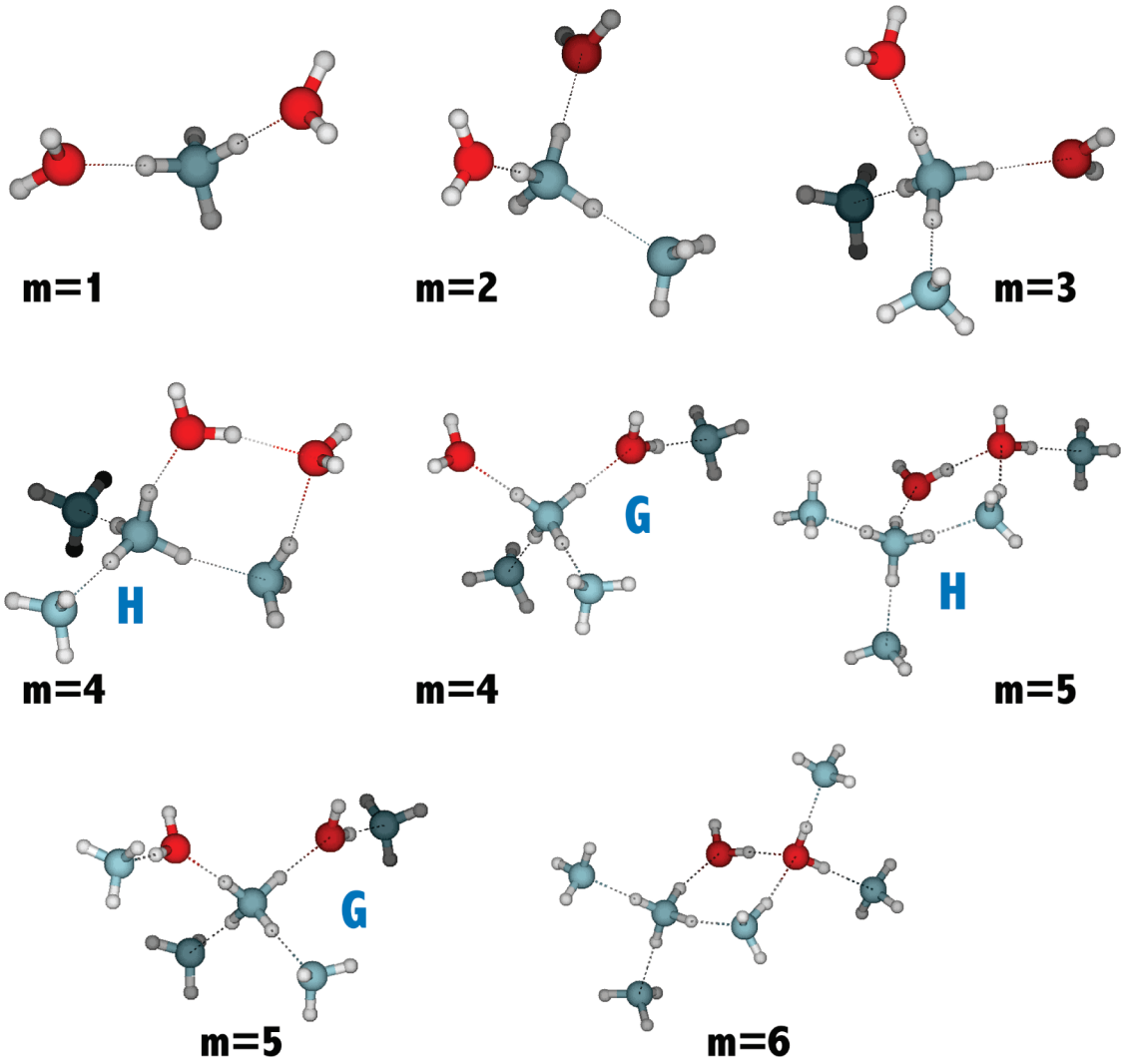

Figure 5. Minimum-enthaply and minimum-free energy structures (at 298 K and 1 atm reference pressure) for $H^+(NH_3)_m(H_2O)_2$ ($m = 1-6$) clusters. In the case that the best structure with respect to the enthalpy (H) and Gibbs free energy (G) were different, both are shown, and the letters "H" and "G" are used to denote the two isomers.

our data show quite interesting features regarding the magic number $H^+(NH_3)_5(H_2O)_{20}$, which will be discussed at the end of this section.

A unique feature of our experiments is the observations made employing CID. In CID some of the mass selected ions are activated by collision, thereby "heating" the ions and inducing dissociation.[49–52] It turns out that CID is very efficient in this respect, and we observe the loss of up to $(m + n)$ ligands. This indicates a very broad energy transfer distribution but typically the peak due to the loss of one ligand dominates, and this is the dissociation which is diagnostic regarding kinetic, and thereby thermodynamic, stability. The experiments showed that mixed clusters containing one ammonia in addition to the magic five, tend to lose this extra ammonia upon CID, while those having five or four tend to lose one water. In other words, the data appear to be in harmony with the idea of a central ammonium surrounded by four ammonia thus forming a common structural motif. However, the mere presence of ions of the types $m = 4$ and 6 in addition to the magic 5—in many instances being more abundant in the magnet scan spectrum—calls for attention and further analysis.

Our quantum chemical calculations do indeed reveal a more complex and chemically richer world than the simplistic geometrical model provides. It turned out that in the case of mixed clusters having one water molecule, there is already a preference for water/ammonia ligand exchange in the first solvation shell. The enthalpy and free energy difference to the thermodynamically less stable $m = 5$ isomer with water in the second shell are 6.5 and 22.9 kJ/mol, respectively. Such ligand exchange is well-known from inorganic chemistry, where, for example, octahedral $Cu(NH_3)_4(H_2O)_4^{2+}$ is a good example.

On the other hand, and despite the fact that the water prefers the first shell, evaporation from ($m = 5$, $n = 1$) is in favor of water loss, in perfect agreement with experiment. In other words, and quite surprisingly, there seems to be no clear-cut relationship between the thermochemically most stable structural arrangement of the ligands and the thermochemistry of evaporation. This is also the conclusion obtained from the computational data for clusters containing two or three water molecules ($n =$ 2 and 3). In some instances up to two of the first shell ligands may be water molecules. It should also be mentioned that the calculations show that clusters with $m = 6$ and above are predicted to lose ammonia in preference to water, also in agreement with experiments. The only slight discrepancy observed is the theoretical prediction that for ($m = 5$, $n = 3$) the enthalpy (but not the free energy) is about 2 kJ/mol in favor of ammonia loss. Experimentally, we observe a 1.3:1.0 preference for water loss, in better accordance with the free energy

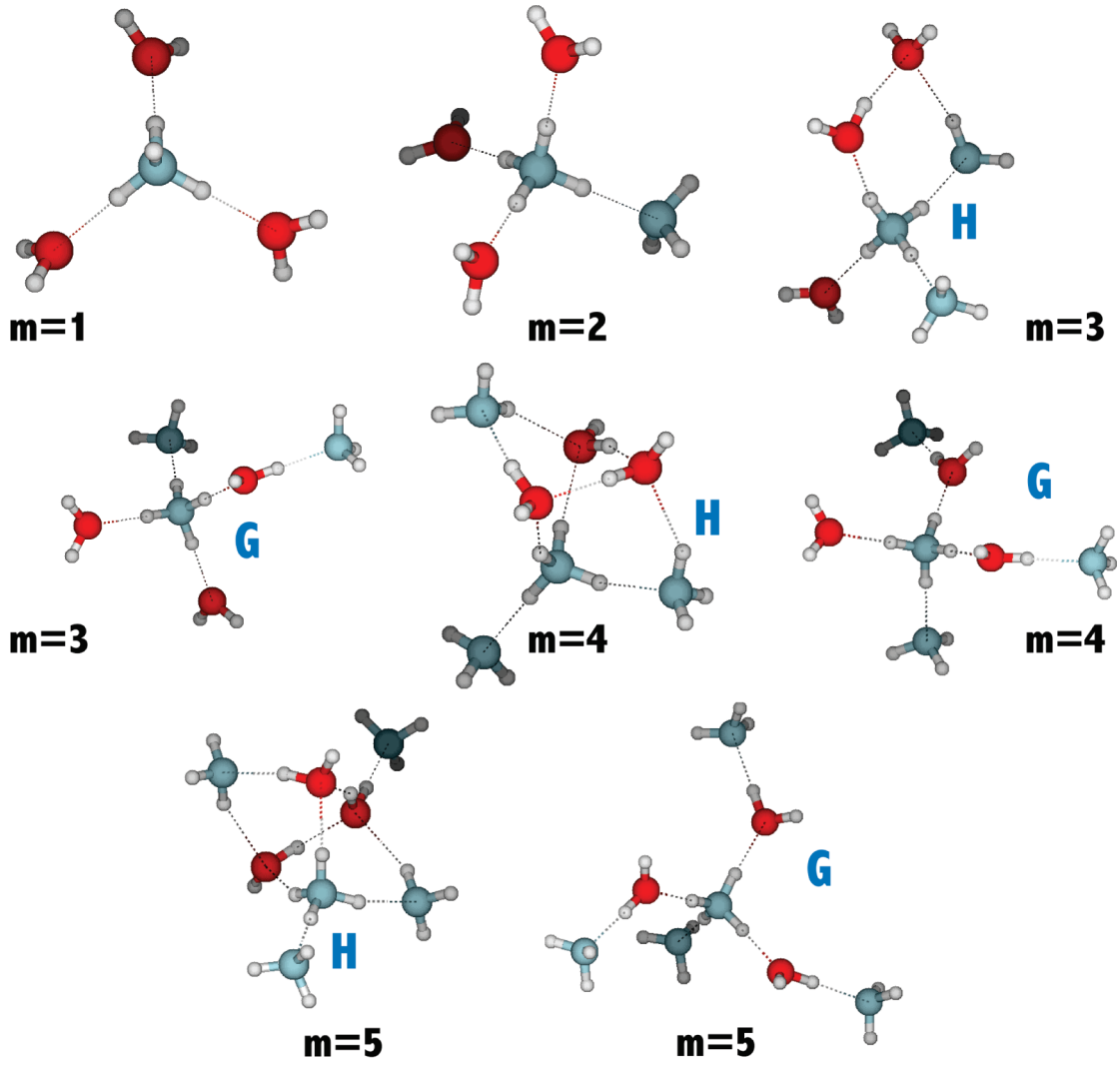

Figure 6. Minimum-enthaply and minimum-free energy structures (at 298 K and 1 atm reference pressure) for $H^+(NH_3)_m(H_2O)_3$ ($m = 1-5$) clusters. In the case that the best structure with respect to the enthalpy (H) and Gibbs free energy (G) were different, both are shown, and the letters "H" and "G" are used to denote the two isomers.

prediction. However, we need to repeat our previous statement regarding the calculations to be reliable at best within 4 kJ/mol.

We note another highly interesting feature in the computational data. According to the calculation, the equilibrium

$$H^+(NH_3)_5 + H_2O \rightleftarrows H^+(NH_3)_4(H_2O) + NH_3$$

is endothermic by 8.7 kJ/mol (2.0 kcal/mol) and endoergic by 2.8 kJ/mol (0.7 kcal/mol), in agreement with the experimental estimates[34,53] of 3 ± 4 kJ/mol and 1 ± 4 kJ/mol, respectively. This means that in the competition between water and ammonia, in an absolute sense, the ammonia molecule preferrably occupies the last position of the first shell, a situation that is different from $H^+(NH_3)_5(H_2O)$ where water is preferred, in the latter case clearly showing the positive influence of an ammonia molecule in the second shell on the stability of the first shell including a water. In any case, we need to consider that the energy differences are rather small, within some kJ/mol.

In discussing the fine details that determine the preferred ligand arrangement in a mixed cluster it is valuable to bear in mind the properties of the compounds that make up the cluster. The enthalpy of vaporation (STP) for water is 44 kJ/mol, and for ammonia it is 20 kJ/mol. This difference is due to the more dipolar character of the O−H bond compared to the N−H bond resulting in stronger hydrogen bond interaction in water, although N is a better acceptor. This indicates much stronger binding in (large) water clusters compared to ammonia clusters, and in the absence of other factors, this would make any attempt to produce mixed clusters very difficult, since water would dominate. However, the considerably higher proton affinity of ammonia—a property that is intimately related to the second moment of the electric field, the polarizability—is decisive in changing the picture by centring the structures around a central ammonium ion. The higher polarizability (equivalently, the proton affinity) of ammonia can also be accounted for in explaining why the first few ligands in these small clusters are ammonia molecules. However, the ion induced force decreases quickly with distance and the charge becomes more disperse with cluster size, resulting in strong H_2O/NH_3 competition already for the last two positions of the first solvation shell around NH_4^+. Beyond the first shell water binding is preferred. Ultimately, this allows for a total maximum of six ammonia molecules. On the other hand, except for the water-free clusters, we observe in no instance less than four ammonia ligands. The dynamic character in allowing water into the first shell but keeping the ammonia close for reinforcement of this situation

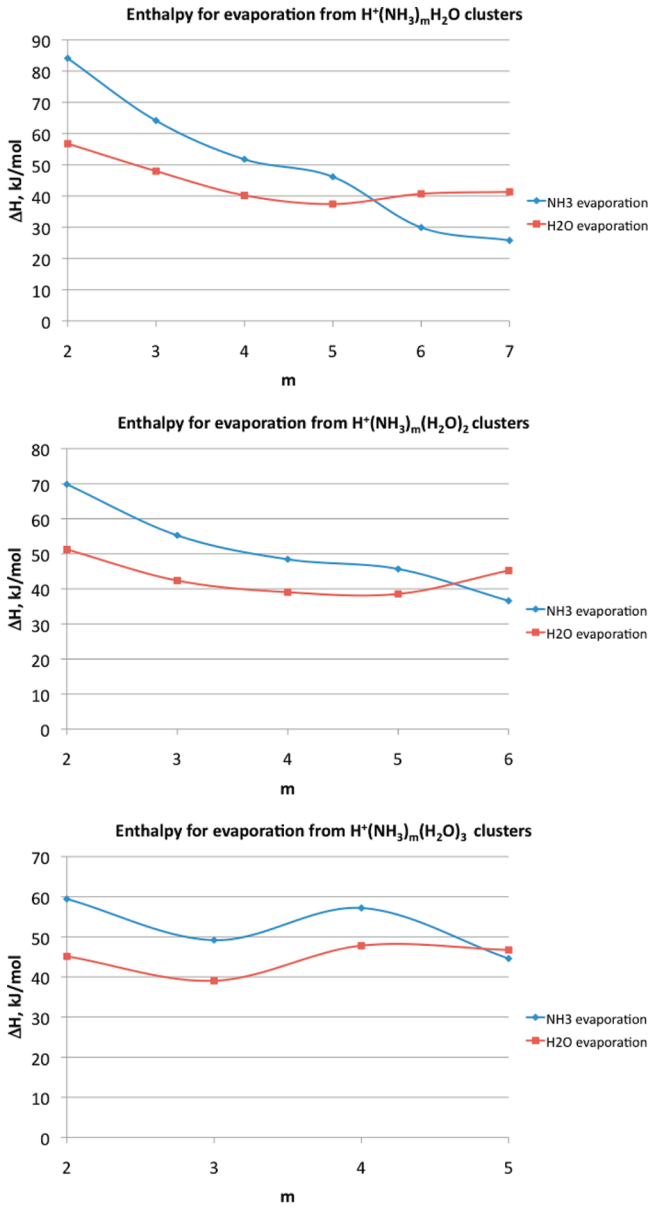

Figure 7. Enthalpies of evaporation (in kJ/mol, at 298 K and 1 atm reference pressure) of ammonia (blue) and water (red) from $H^+(NH_3)_mH_2O$ (top), $H^+(NH_3)_m(H_2O)_2$ (middle), and $H^+(NH_3)_m(H_2O)_3$ (bottom) clusters.

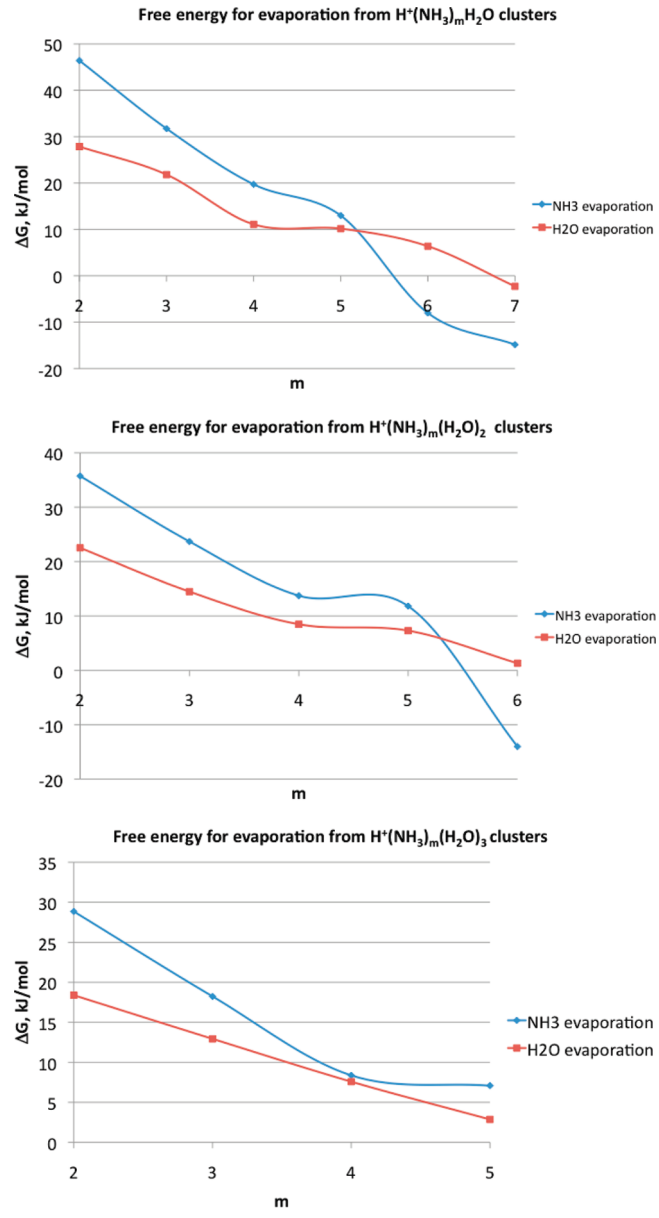

Figure 8. Gibbs free energies of evaporation (in kJ/mol, at 298 K and 1 atm reference pressure) of ammonia (blue) and water (red) from $H^+(NH_3)_mH_2O$ (top), $H^+(NH_3)_m(H_2O)_2$ (middle), and $H^+(NH_3)_m(H_2O)_3$ (bottom) clusters.

seems to be the key. The dynamics of ligand swapping within the first and second shells is probably fast, and a number of energetically low-lying isomeric clusters structures will be populated at room temperature. However, the temperature sinks upon evaporation, leading to slower ligand exchange dynamics and ultimately to a freezing out of the isomer lowest in enthalpy. In all computed structures, the proton is attached to a central ammonia molecule. This will most likely be the case also for slightly larger clusters, since proton mobility from ammonium to water is low, as observed in isotope exchange experiments with $H^+(NH_3)(H_2O)_n$ ($n < 30$).[28] For larger clusters, we have good reason to expect that proton mobility will increase, simply due to the fact that the proton affinity of a water cluster increases with size, overtaking the proton affinity of the single ammonia molecule already around $n = 4$.[54] This is also to be expected when taking the acidity of the ammonium ion in bulk solution into consideration. The conclusion to be drawn from the last part of this discussion is that the structure of large mixed ammonia/water clusters at room temperature is in flux, having relatively few fixed features, while at lower temperatures, upon approaching the solid state, the structure may become a more meaningful concept.

Finally, we want to include a few comments on the magic number species $H^+(NH_3)_5(H_2O)_{20}$. It may appear more than coincidental that this enhanced stability cluster combines the magic numbers of the tetrahedral $H^+(NH_3)_5$ and the dodecahedral $(H_2O)_{20}$. However, in the preceding we have moved very close to the myth-busting position that there is relatively little magic about these Platonic structures in the context of water/ammonia cluster chemistry. Despite this, the geometric hypothesis deserves to be tested out also in this case. Unfortunately, the cluster is too big to be treated at a high computational level. We have therefore limited ourselves to applying the semiempirical PM3 method[55,56] for the purpose of illustration. In the geometry optimized $(H_2O)_{20}$ cage, the distance between diametrically opposed oxygen atoms (between 7.6 and 7.7 Å) is too small to host a complete $H^+(NH_3)_5$ entity without causing

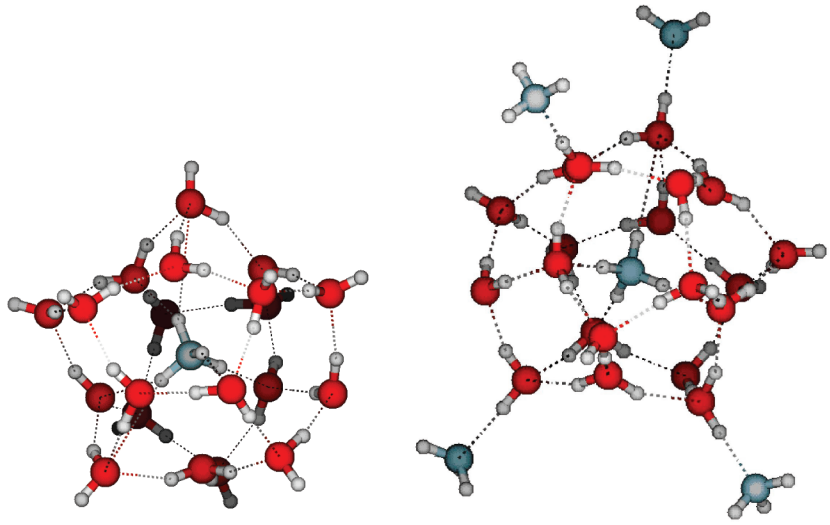

Figure 9. Putative structures of the $H^+(NH_3)(H_2O)_{20}$ and $H^+(NH_3)_5(H_2O)_{20}$ clusters, optimized at the PM3 level.

significant structural distortion of the perfect dodecahedron, although it is too large to host a single ammonium ion in a space filling fashion, as previously suggested.[36] Having one ammonia inside and the rest on the outside would correspond to the extreme situation where all four ammonia molecules of the first shell have been displaced but where they compensate by reinforcing the total structure. The two geometry-optimized structures are shown in Figure 9. In the rightmost structure we note that this particular $H^+(NH_3)(H_2O)_{20}$ structure contains four symmetrical binding sites for ammonia addition immediately outside the first all-water shell. Quantitative exploration of this effect would require more advanced configurational sampling methods, and more computer power, than currently available.

Conclusion

The present study supports the idea that small protonated mixed clusters of NH_3 and H_2O contain a central NH_4^+ core. However, and contrary to general belief, the particular stability of clusters having five ammonia molecules is not due to a particular stable tetrahedral arrangement of four equivalent ammonia molecules directly connected to the core ion via hydrogen bonds. Instead, water and ammonia molecules compete for sites in the first and second solvation shell on an approximately equal footing. As it turns out, the enhanced stability of clusters sizes of enhanced stability, having so-called magic numbers, can in general not be linked to particular static geometric arrangements of high symmetry. Future experimental and computational efforts are needed to provide even better insight into this fascinating question.

Acknowledgment. The authors appreciate the support to this research project from European Project ITS LEIF (RII3/026015), and the experiments were performed at the Sep1 facility, part of the distributed ITS LEIF infrastructure. Thanks to Professor Dr. Bernd Hartke, Kiel, for providing water cluster geometries. P. H., K. S. and S. B. N. also gratefully acknowledge support from Lundbeckfonden. T. K. would like to thank the Academy of Finland for funding and the CSC IT Centre for Science in Espoo, Finland, for computer time. M. J. R. is grateful to the Swedish Research Council, the Nanoparticle in Interactive Environments platform at the Faculty of Science at University of Gothenburg. E. U. acknowledges the Norwegian Research Council by the Grant No. 179568/V30 to the Centre of Theoretical and Computational Chemistry through their Centre of Excellence program and NOTUR for generous computational resources.

Supporting Information Available: Table containing absolute energies, enthalpies and Gibbs free energies plus Cartesian coordinates of all species reported. This material is available free of charge via the Internet at http://pubs.acs.org.

References and Notes

(1) Chaplin, M. F., Water Structure and Science, http://www1.lsbu.ac.uk/water/. With 1626 references (as of January2010).
(2) Castleman, A. W.; Bowen, K. H. *J. Phys. Chem.* **1996**, *100*, 12911.
(3) Kebarle, P. *Int. J. Mass Spectrom.* **2000**, *200*, 313.
(4) Kulmala, M.; Vehkamäki, H.; Petäjä, T.; Dal Maso, M.; Lauri, A.; Kerminen, V. M.; Birmili, W.; McMurry, P. H. *J. Aerosol Sci* **2004**, *35*, 143.
(5) Kulmala, M.; Asmi, A.; Lappalainen, H. K.; Carslaw, K. S.; Pöschl, U.; Baltensperger, U.; Hov, Ø.; Brenquier, J.-L.; Pandis, S. N.; Facchini, M. C.; Hansson, H.-C.; Wiedensohler, A.; O'Dowd, C. D. *Atmos. Chem. Phys.* **2009**, *9*, 2825.
(6) Yu, F.; Turco, R. P. *Geophys. Res. Lett.* **2000**, *27*, 883.
(7) Wayne, R. P. *Chemistry of Atmospheres*; Oxford University Press Inc: New York, 2000.
(8) Marsh, N. D.; Svensmark, H. *Phys. Rev. Lett.* **2000**, *85*, 5004.
(9) Perkins, M. D.; Eisele, F. L. *J. Geophys. Res.* **1984**, *89*, 9649.
(10) Arnold, F.; Wohlfrom, K. H.; Schneider, J.; Klemm, M.; Stilp, T.; Grimm, F. *J. Aerosol Sci* **1997**, *28*, S65.
(11) Ball, S. M.; Hanson, D. R.; Eisele, F. L.; McMurry, P. H. *J. Geophys. Res.* , *104*.
(12) Kebarle, P.; Hogg, A. M. *J. Chem. Phys.* **1965**, *42*, 798.
(13) Hogg, A. M.; Kebarle, P. *J. Chem. Phys.* **1965**, *43*, 449.
(14) Payzant, J. D.; Cunningham, A. J.; Kebarle, P. *Can. J. Chem.* **1973**, *51*, 3242.
(15) Arshadi, M. R.; Futrell, J. H. *J. Phys. Chem.* **1974**, *78*, 1482.
(16) Tang, I. N.; A. W.; Castleman, J. *J. Chem. Phys.* **1975**, *62*, 4576.
(17) Schwarz, H. A. *J. Chem. Phys.* **1980**, *72*, 284.
(18) Price, J. M.; Crofton, M. W.; Lee, Y. T. *J. Phys. Chem.* **1991**, *95*, 2182.
(19) Tono, K.; Fukazawa, K.; Tada, M.; Fukushima, N.; Tsukiyama, K. *Chem. Phys. Lett.* **2007**, *442*, 206.
(20) Hirao, K.; Fujikawa, T.; Konishi, H.; Yamabe, S. *Chem. Phys. Lett.* **1984**, *104*, 184.
(21) Nakai, H.; Goto, T.; Ichikawa, T.; Okada, Y.; Orii, T.; Takeuchi, K. *Chem. Phys.* **2000**, *262*, 201.
(22) Nakai, H.; Goto, T.; Okada, Y.; Orii, T.; Takeuchi, K.; Ichihashi, M.; Kondow, T. *J. Chem. Phys.* **2000**, *112*, 7409.
(23) Wang, B.-C.; Chang, J.-C.; Jiang, J.-C.; Lin, S.-H. *Chem. Phys.* **2002**, *276*, 93.
(24) Miyazaki, M.; Fujii, A.; Ebata, T.; Mikami, N. *Science* **2004**, *304*, 1134.

(25) Headrick, J. M.; Diken, E. G.; Walters, R. S.; Hammer, N. I.; Christie, R. A.; Cui, J.; Myshakin, E. M.; Duncan, M. A.; Johnson, M. A.; Jordan, K. D. *Science* **2005**, *308*, 1765.
(26) Hartke, B. *Angew. Chem., Int. Ed.* **2002**, *41*, 1468.
(27) Marx, D.; Tuckerman, M. E.; Hutter, J.; Parrinello, M. *Nature* **1999**, *397*, 601.
(28) Andersson, P. U.; Ryding, M. J.; Sekiguchi, O.; Uggerud, E. *Phys. Chem. Chem. Phys.* **2008**, *10*, 6127.
(29) Lin, S.-S. *Rev. Sci. Instrum.* **1973**, *44*, 516.
(30) Searcy, J. Q.; Fenn, J. B. *J. Chem. Phys.* **1974**, *61*, 5282.
(31) Hodges, M. P.; Wales, D. J. *Chem. Phys. Lett.* **2000**, *324*, 279.
(32) James, T.; Wales, D. J.; Hernandez-Rojas, J. *Chem. Phys. Lett.* **2005**, *415*, 302.
(33) Iyengar, S. S.; Petersen, M. K.; Day, T. J. F.; Burnham, C. J.; Teige, V. E.; Voth, G. A. *J. Chem. Phys.* **2005**, *123*, 084309.
(34) Payzant, J. D.; Cunningham, A. J.; Kebarle, P. *Can. J. Chem.* **1973**, *51*, 3242.
(35) Jiang, J. C.; Chang, H. C.; Lee, Y. T.; Lin, S. H. *J. Phys. Chem. A.* **1999**, *103*, 3123.
(36) Shinohara, H.; Nagashima, U.; Tanaka, H.; Nishi, N. *J. Chem. Phys.* **1985**, *83*, 4183.
(37) Shinohara, H.; Nagashima, U.; Nishi, N. *Chem. Phys. Lett.* **1984**, *111*, 511.
(38) Shinohara, H.; Nishi, N.; Washida, N. *Chem. Phys. Lett.* **1988**, *153*, 417.
(39) Boltalina, O. V.; Hvelplund, P.; Jørgensen, T. J. D.; Larsen, M. C.; Larsson, M. O.; Sharoitchenko, D. A. *Phys. Rev. A* **2000**, *62*, 023202.
(40) Larsson, M. O.; Hvelplund, P.; Larsen, M. C.; Shen, H.; Cederquist, H.; Schmidt, H. T. *Int. J. Mass Spectrom.* **1998**, *177*, 51.
(41) Drenck, K.; Hvelplund, P.; Nielsen, S. B.; Panja, S.; Støchkel, K. *Int. J. Mass Spectrom.* **2008**, *273*, 126.
(42) Sundén, A. E. K.; Støchkel, K.; Panja, S.; Kadhane, U.; Hvelplund, P.; Nielsen, S. B.; Zettergren, H.; Dynefors, B.; Hansen, K. *J. Chem. Phys.* **2009**, *130*, 224308.
(43) Frisch, M. J.; Trucks, G. W.; Schlegel, H. B.; Scuseria, G. E.; Robb, M. A.; Cheeseman, J. R.; Montgomery, J. A., Jr.; Vreven, T.; Kudin, K. N.; Burant, J. C.; Millam, J. M.; Iyengar, S. S.; Tomasi, J.; Barone, V.; Mennucci, B.; Cossi, M.; Scalmani, G.; Rega, N.; Petersson, G. A.; Nakatsuji, H.; Hada, M.; Ehara, M.; Toyota, K.; Fukuda, R.; Hasegawa, J.; Ishida, M.; Nakajima, T.; Honda, Y.; Kitao, O.; Nakai, H.; Klene, M.; Li, X.; Knox, J. E.; Hratchian, H. P.; Cross, J. B.; Bakken, V.; Adamo, C.; Jaramillo, J.; Gomperts, R.; Stratmann, R. E.; Yazyev, O.; Austin, A. J.; Cammi, R.; Pomelli, C.; Ochterski, J. W.; Ayala, P. Y.; Morokuma, K.; Voth, G. A.; Salvador, P.; Dannenberg, J. J.; Zakrzewski, V. G.; Dapprich, S.; Daniels, A. D.; Strain, M. C.; Farkas, O.; Malick, D. K.; Rabuck, A. D.; Raghavachari, K.; Foresman, J. B.; Ortiz, J. V.; Cui, Q.; Baboul, A. G.; Clifford, S.; Cioslowski, J.; Stefanov, B. B.; Liu, G.; Liashenko, A.; Piskorz, P.; Komaromi, I.; Martin, R. L.; Fox, D. J.; Keith, T.; Al.Laham, M. A.; Peng, C. Y.; Nanayakkara, A.; Challacombe, M.; Gill, P. M. W.; Johnson, B.; Chen, W.; Wong, M. W.; Gonzalez, C.; Pople, J. A. *Gaussian 09*; Gaussian, Inc.: Wallingford CT, 2009.
(44) Montgomery, J. A., Jr.; Frisch, M. J.; Ochterski, J. W.; Petersson, G. A. *J. Chem. Phys.* **1999**, *110*, 2822.
(45) Montgomery, J. A., Jr.; Frisch, M. J.; Ochterski, J. W.; Petersson, G. A. *J. Chem. Phys.* **2000**, *112*, 6532.
(46) Nielsen, S. B.; Masella, M.; Kebarle, P. *J. Phys. Chem. A.* **1999**, *103*, 9891.
(47) Hansen, K.; Andersson, P. U.; Uggerud, E. *J. Chem. Phys.* **2009**, *131*, 124303.
(48) Klots, C. E. *Z. Phys. D.* **1987**, *5*, 83.
(49) Cooper, H. J.; Derrick, P. J.; Jenkins, H. D. B.; Uggerud, E. *J. Phys. Chem.* **1993**, *97*, 5443.
(50) Uggerud, E.; Derrick, P. J. *J. Phys. Chem.* **1991**, *95*, 1430.
(51) Wysocki, V. H.; Kenttämaa, H. I.; Cooks, R. G. *Int. J. Mass Spectrom. Ion Proc.* **1987**, *75*, 181.
(52) Pollreisz, F.; Gömöry, Á.; Sztáray, J.; Végh, P.; Drahos, L.; Kiss, A.; Vékey, K. *Int. J. Mass Spectrom.* **2005**, *243*, 41.
(53) Lias, S. G.; Rosenstock, H. M.; Deard, K.; Steiner, B. W.; Herron, J. T.; Holmes, J. H.; Levin, R. D.; Liebman, J. F.; Kafafi, S. A.; Bartmess, J. E.; Hunter, E. F. In NIST Chemistry Webbok; http://webbook.nist.goc/chemistry, 2010.
(54) Uggerud, E. *Int. J. Mass Spectrom.* **1999**, *182*−*183*, 13.
(55) Stewart, J. J. P. *J. Comput. Chem.* **1989**, *10*, 209.
(56) Stewart, J. J. P. *J. Comput. Chem.* **1989**, *10*, 221.

JP104162K